RSC Advances

ROYAL SOCIETY OF CHEMISTRY

www.rsc.org/advances

Cite this: DOI: 10.1039/c0xx00000x

www.rsc.org/xxxxxx

ARTICLE TYPE

Continuous Sol–Gel Derived SiOC/HfO_2 Fibers with High–Strength

Yao Xu,[a] Dong Su,*[a] Hongjun Feng,[a] Xiao Yan,*[a,b] Ning Liu[a]

Received (in XXX, XXX) Xth XXXXXXXXX 20XX, Accepted Xth XXXXXXXXX 20XX
DOI: 10.1039/b000000x

This study presents fabrication and characterization of continuous SiOC/HfO_2 fibers with high-strength by sol–gel process. Continuous polyhafnosiloxane (PHfSO) gel fibers are spun from the solution of silicon alkoxides and hafnium dichloride using polyvinyl pyrrolidone as spinning reagent, and then transform into dense SiOC/HfO_2 fibers with homogeneous shrinkage by subsequent drying and pyrolysis treatment. Fourier transform infrared and X-ray photoelectron spectra together with X-ray diffraction analysis indicate that the amorphous SiOC/HfO_2 fibers consist of mixed silicon oxycarbide (SiO_xC_{4-x}, x=1–4) and tetravalent hafnium-oxygen units embraced with certain free-carbon phase. Scanning electron microscopy and transmission electron microscopy observation reveal that the SiOC/HfO_2 fibers with homogenous Hf distribution exhibit circular–shaped or elliptical–shaped cross-section depending on their thickness when as gel fibers. Mechanical testing shows that the SiOC/HfO_2 fibers exhibit good mechanical property with maximum tensile strength of 1.5 GPa arising from the incorporation of Hf in the SiOC network.

Introduction

Hafnium–containing polymer–derived ceramics (for instance SiHfCNO [1–4], SiOC/HfO_2 [5–8]) have excellent thermal stability [6], oxidation resistance [1,4] and crystallization resistance [2,5,6], making them promising candidates as thermal and environmental protection barriers in the high–temperature field of energy, environment and transportation. Moreover, they have great application potential in nuclear industry and electronic field due to their absorptive nuclear capacity and high dielectric constant. [2,6]

The SiOC/HfO_2 ceramics exhibit remarkably improved thermal stability up to 1600°C compared with Hf–free SiOC ceramic [6] and have been synthesized from hafnium modified polysiloxanes (PSO) precursors through polymer-to-ceramic transformation process. They exhibit single Si–Hf–O–C phase at low temperatures below 1000°C, and subsequently converted into SiOC/HfO_2 nanocomposites through phase separation under high-temperature annealing. [5,7] The microstructure and pyrolysis behavior of Hf–containing PSO precursor, structural changes, phase evolution, microstructure evolution and high–temperature stability of SiOC/HfO_2 ceramics have been systematically studied in recent years [5–8]. Yet relevant studies on SiOC/HfO_2 fiber materials are still limited.

Sol–gel process can not only easily incorporate Hf into SiOC utilizing the hydrolysis and condensation reaction of hafnium alkoxides/salts and silicon alkoxides, but also allow for spinning of fiber materials from the sol or solution by adjusting its molecular structure, viscosity and rheological property. In this work, continuous SiOC/HfO_2 fibers have been successfully fabricated from ethanol solution of $HfOCl_2$ and silicon alkoxide precursors using sol–gel method through spinning, drying and pyrolysis. The fiber compositions, chemical structures and morphologies were studied together with their mechanical properties.

Experimental

Hafnium dichloride oxide octahydrate ($HfOCl_2{\cdot}8H_2O$, ABCR GmbH & Co. KG) was used as hafnium source, while tetraethoxysilane (TEOS, $Si(OC_2H_5)_4$, Tianjin Jiangtian Co. Ltd., Tianjin, China) and dimethyldiethoxylsilane (DMDES, $Si(CH_3)_2(OC_2H_5)_2$, Shanghai Yumei Co. Ltd., Shanghai, China) were used as silicon alkoxide precursors. Polyvinyl pyrrolidone (PVP, $-[C_6H_9NO]_n-$, K30, Tianjin Jiangtian Co. Ltd., Tianjin, China), which are widely used in fabricating ceramic fibers such as Al_2O_3 and mullite fibers as well as in electrospinning [9,10], was used as spinning reagent. The average molecular weight of PVP is 50000 with the polymerization degree (n) of ~450. Ethanol (CH_3CH_2OH, Tianjin Jiangtian Co. Ltd., Tianjin, China) was used as solvent.

In a typical experiment, TEOS (2.08 g, 10 mmol), DMDES (2.88 g, 20 mmol), water (0.32 g, 18 mmol), ethanol (2 g) and $HfOCl_2{\cdot}8H_2O$ (0.24 g, 0.6 mmol) were charged sequentially in a beaker mixed under magnetic stirring to form transparent solution, and then PVP (0.70 g) was added to form viscous solution by stirring for ~1h. The spinnablity of the solution was evaluated by continuous dipping a glass bar in it until a 5 cm-length fiber can be drawn. The viscosity of the spinnable solution was in the range of 10 - 150 p according to the viscosity measurement at 25 °C under a rotating velocity of 25 r/min. Polyhafnosiloxane (PHfSO) gel fibers were hand-drawn from the solution with a glass bar at velocity of 5-10 cm/s, and then dried at 50 °C for 5 h. The PHfSO gel fibers were converted to SiOC/HfO_2 ceramic fibers by pyrolysis at 1000 °C for 1 h at a ramp of 5 °C/min in flowing argon.

The chemical structures of the PHfSO fibers and the SiHfOC fibers were characterized by Fourier transform infrared spectroscopy (FTIR, Rayleigh WQF-510, Beijing, China) in the

frequency range of 400–4000 cm^{-1} using standard KBr pellet technique. Their surface chemical compositions and structures were detected by X-ray photoelectron spectroscopy (XPS, K-alpha, ThermovFisher Scientific, East Grinstead, UK) using Al *Kα* X-ray source as excitation source on the analyzed area with a diameter of about 400 μm. Phase analysis was performed on X-ray diffractometer (XRD, Rigaku D/max 2500 v/pc, Tokyo, Japan) using Cu *Kα* radiations (λ = 1.54 Å) in the range of 10-90° at scanning rate of 5°/min. The morphologies of the PHfSO fibers and the SiHfOC fibers were observed by scanning electron microscopy (SEM, s4800, Hitachi, Japan) after gold coating and transmission electron microscopy (TEM, Tecnai G2 F20, Philips, Eindhoven, the Netherlands). The accelerating voltage of 5 kV and secondary electron mode were exploited in SEM observation. The pyrolysis behavior of PHfSO fibers was analyzed by thermal gravimetric analysis (TGA, NETZSCH STA 449F3, Waldkraiburg, Germany) under flowing argon with a heating rate of 10 °C/min up to 1000 °C (sample mass: about 10 mg). Tensile tests were conducted on a fiber microtester (JSF08, Shanghai Zhongchen Co. Ltd., Shanghai, China) with 2 mm gauge length at strain rate of 0.3 mm/min.

Results and Discussion

$HfOCl_2$ is used as the hafnium source and the acid catalysis in our spinning sol–gel system. Hydrolysis of $HfOCl_2$ provides HCl catalyzing the hydrolysis of TEOS and DMDES while Hf is incorporated into polysiloxane (PSO) network through condensation between hafnium hydrolysates and silicon hydrolysates, therefore no additional catalyst is needed in this system. *In-situ* HCl catalyzed sol–gel system makes it easy to realize the fiber drawing since linear structure molecules are preferentially formed in acid condition [11–13]. The amount of $HfOCl_2$ is critical on fiber spinning and the mole ratio of $HfOCl_2$/ALK (ALK=TEOS+DMDES) should be lower than 0.05. Two factors contribute to this: 1) formation of branched molecules and 2) decrease solubility of the PVP in the solution. Firstly, too much $HfOCl_2$ will increase the HCl concentration and therefore cause silicon alkoxides to form some branched structures rather than linear structures [11–13], which is detrimental to fiber drawing. Secondly, the solubility of PVP in ethanol decreases with increasing $HfOCl_2$, which leads to phase separation and affects the fiber spinning.

Solutions with various compositions were prepared with the mole ratio $HfOCl_2$/ALK=0.01-0.1 and PVP/ALK=0.1-0.4, and the optimal mole ratios of $HfOCl_2$/ALK and PVP/ALK were 0.02 and 0.2 respectively. Under this condition, the solution shows excellent spinnability and stability, tens of meters long PHfSO fibers with smooth surface are obtained. The fibers are white, flexible and monodispersed (Fig. 1a and b). The fibers are 5-60 μm thick, which should be closely related to the sol viscosity and spinning speed according to experimental observation. Hand-drawn fibers do not have a constant diameter or a unique shape in cross-section. They show circular- or elliptical-shaped cross-section depending on the thickness as determined from observation on 50 fibers (circular: <20 μm, Fig.1c; elliptical: >30 μm, Fig. 1d). The out-of-round shape of the thicker fibers is attributed to the non-homogeneous shrinkage and collapse during gelation and drying, as previously observed in the silica gel fibers drawn from a TEOS solution [12].

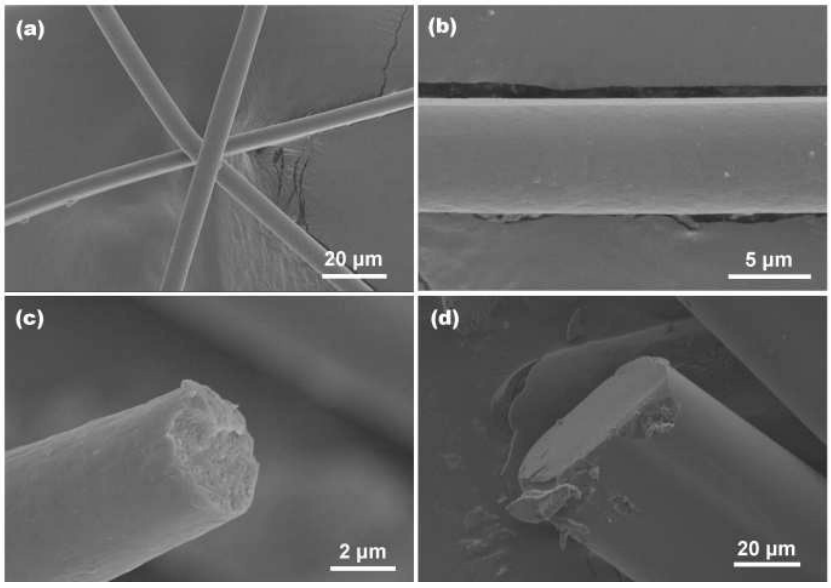

Fig. 1 SEM images of PHfSO gel fibers: (a)monodispersed fibers, (b) enlarged image of a fiber surface, (c) circular-shaped fiber and (d) elliptical-shaped fiber.

The composition and surface chemical structure of PHfSO fibers are analyzed by XPS. The signals are detected for Si, O, C, N and Hf (Fig.2a) with respective percentage of 18.4, 27.9, 49.5, 3.5 and 0.7 at.% corresponding to formula of $SiHf_{0.04}O_{1.52}C_{2.69}N_{0.20}$. Si2p, C1s and Hf4f peak fittings are given in Fig.2b–d in order to illustrate the corresponding components of PHfSO fibers. The Si2p peak suggests the presence of SiO_4 and C_2SiO_2 units at 103.3 and 102.2 eV [14,15] respectively. The C1s peak shows a predominant peak at 284.8 eV, which is assigned to CH_3 units [14,15] corresponding to the methyl groups of DMDES and PVP. Moreover, there are two weak peaks at 288.2 and 286.2 eV [14,15] due respectively to C=O and CH/CH_2 units arising from the PVP. The $Hf4f_{5/2}$ and $Hf4f_{7/2}$ peaks at 19.2 and 17.5 eV with area ratio of 3: 4 can be assigned to HfO_2 (IV). The higher bonding energy of Hf–O compared with that of reported HfO_2 ($Hf4f_{5/2}$ and $Hf4f_{7/2}$: 18.4 and 16.7 eV respectively [16]) may result from the existence of Hf–O–Si units in the fibers. FTIR (Fig. 3) spectrum shows that Hf–O–Si vibration[5] appears at ~950 cm^{-1}

indicating Hf has been incorporated into Si–O tetrahedron through the co-condensation of $HfOCl_2$ and silicon alkoxides. The formation of Hf–O–Si makes the Hf4f peak shift toward high binding energy due to lower electronegativity of Hf than Si. In the FTIR spectra, an intense broad band at 1090 cm^{-1} can be assigned to the Si–O–Si stretching vibration arising from the condensation units of DMDES and TEOS. The sharp peaks at 1272, 847 and 800 cm^{-1} can be respectively assigned to the bending, rocking and stretching vibration of Si–Me[17] corresponding silicon atoms sharing bonds with two methyl units (–$Si(Me)_2$–) from DMDES, and the C–H stretching vibration appears at ~2900 cm^{-1}. The peak at 1661 cm^{-1} can be assigned to the stretching vibration of C=O from PVP. Therefore, PHfSO fibers should mainly consist of SiO_4 and C_2SiO_2 units with the incorporation of Hf in the form of Hf–O–Si and Hf–O–Hf.

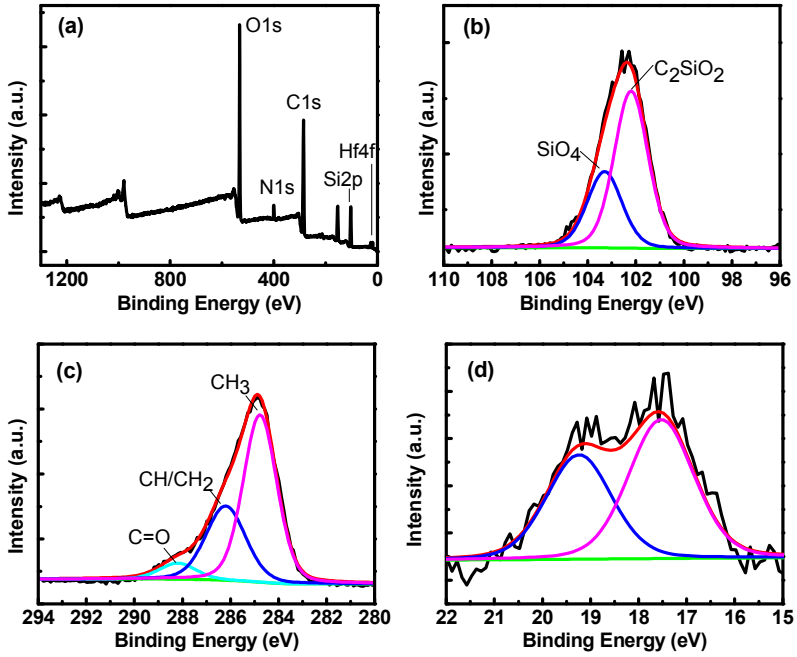

Fig.2 XPS spectrum of PHfSO gel fibers (a) and their Si2p (b), C1s (c) and Hf4f (d) peak fittings.

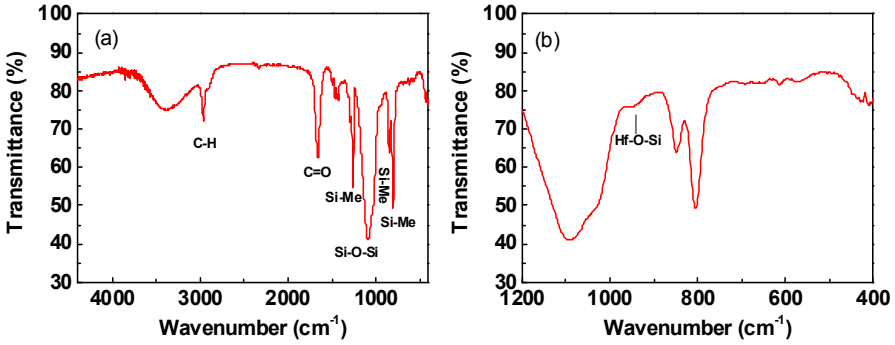

Fig. 3 (a) FTIR spectrum of the PHfSO fibers. (b) Enlarged detail in the range of 1200-400 cm^{-1}.

Pyrolysis behavior of the PHfSO fibers was analyzed by TGA and the data are presented in Fig. 4. The TGA results show three stages of weight loss: 11 wt.% between 142 and 372 °C, 22 wt.% between 372 and 460 °C, and 17 wt.% between 460 and 800 °C. The total weight loss is 50 wt.%, corresponding to a ceramic yield of 50 wt.%. The small weight loss at the initial stage results from the releasing of small molecules and/or some oligomers, such as alcohol and water[18,19]. The large weight loss (22 wt.%) at the second stage is mainly due to thermal degradation and evaporation of the PVP during the heating and a distinct exothermic peak of PVP appears at 425 °C. The third stage corresponds to the stage of organic-to-inorganic transformation from PHfSO gel to SiHfOC ceramic accompanying with the releasing of hydrocarbons and hydrogen and the structural rearrangement of Si–C and Si–O bond as sol-gel derived SiOC[18,19]

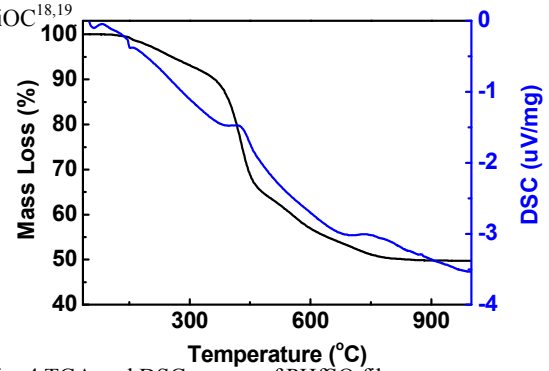

Fig. 4 TGA and DSC curves of PHfSO fiber

PHfSO gel fibers are transformed to $SiOC/HfO_2$ ceramic fibers without cracking after drying at 50 °C for 5 h and pyrolysis at 1000 °C for 1 h in argon. XRD analysis shows the obtained $SiOC/HfO_2$ fibers are amorphous without the formation of SiC, SiO_2 or HfO_2 nanocrystallites, as shown in Fig.5a. The $SiOC/HfO_2$ fibers are dense from SEM observation on both surface and cross-section (Fig. 6 a and b), indicating the PVP addition does not bring in pores in the fibers after pyrolysis. The $SiOC/HfO_2$ fibers retain the circular-shaped cross-section for the thin ones (Fig. 6c) and elliptical-shaped cross-section for the thick ones (Fig. 6d) but with a smaller thickness of 4~55 μm indicating the homogeneous shrinkage during pyrolysis. The shrinkage of the fibers after pyrolysis is due to the structure adjustment during the organic-to-inorganic transformation, which is similar to the shrinkage of the polymer-derived ceramics during pyrolysis. High-resolution TEM (Fig. 7) observation reveals the $SiOC/HfO_2$ fiber is fully amorphous and no clear evidence for SiC and HfO_2 nanocrystallites, which is consistent with XRD analysis. Energy-filtered elemental mapping analysis show Si, C, O and Hf are homogenous distributed in fibers without agglomeration of Hf (Fig.8).

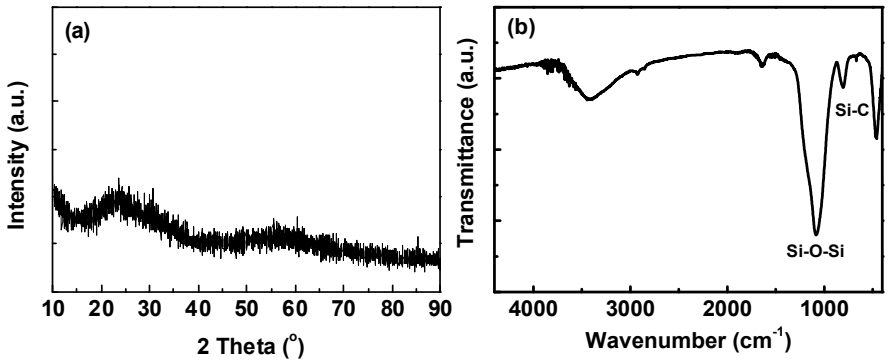

Fig. 5 XRD (a) and FTIR (b) spectra of $SiOC/HfO_2$ fibers from PHfSO fibers pyrolyzed at 1000 °C for 1 h in argon

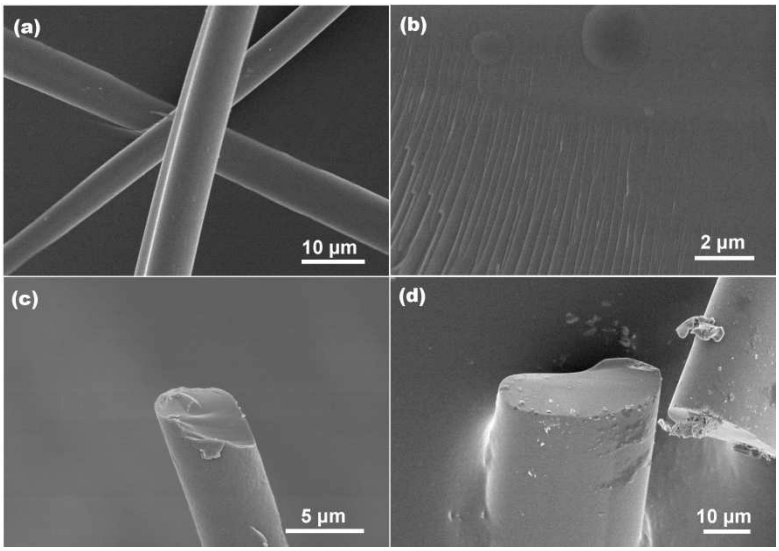

Fig.6 SEM images of $SiOC/HfO_2$ fibers from PHfSO fibers pyrolyzed at 1000 °C for 1 h in argon. (a) monodispersed fibers, (b) dense cross-section, (c) circular-shaped fiber and (d) elliptical-shaped fiber.

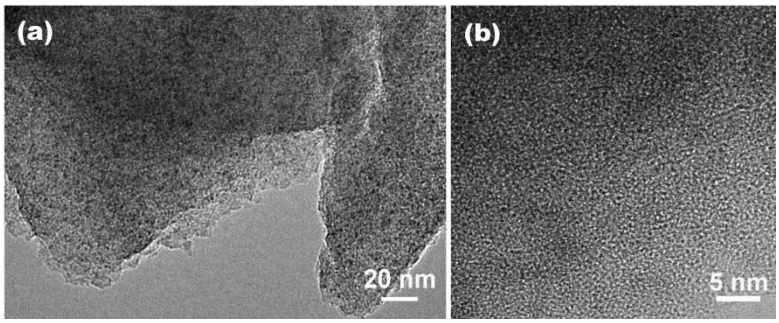

Fig. 7 High-solution TEM image of $SiOC/HfO_2$ fiber pyrolyzed at 1000 °C for 1 h in argon

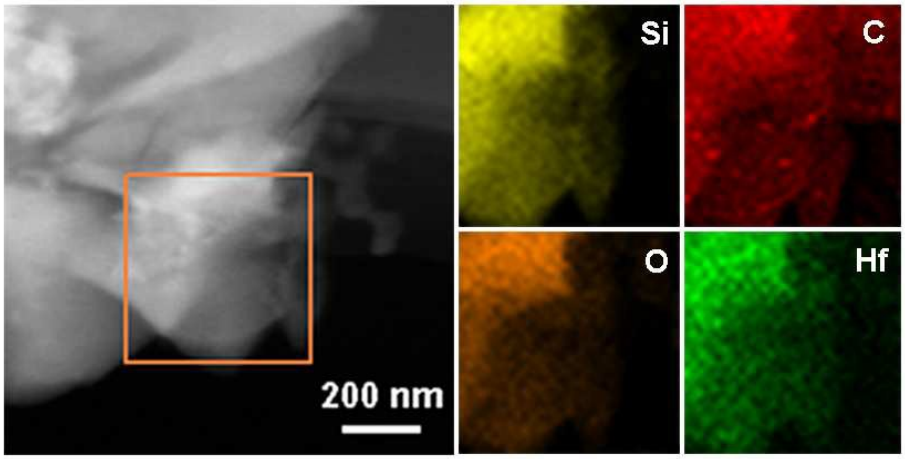

Fig.8 Energy filtered elemental maps of SiOC/HfO_2 fiber pyrolyzed at 1000 °C for 1 h in argon

The SiOC/HfO_2 fibers consist of Si, O, C and Hf with the percentage of 27.7, 43.2, 28.8 and 0.3 at.%, corresponding to empirical formula of $SiHf_{0.01}O_{1.56}C_{1.04}$ as calculated from XPS results (Fig.9a). No nitrogen is detected in the fibers further confirming the complete decomposition of PVP after pyrolysis. The carbon content decreases from 49.5 at.% to 28.8 at.% due to decomposition of the hydrocarbon groups during organic-to-inorganic transformation, which is consistent with the FTIR and TGA results. Si2p peak (Fig.9b) is assigned to the presence of mixed silicon oxycarbide units such as SiO_4(105.0 eV), $CSiO_3$(104.1 eV), C_2SiO_2(103.3 eV) and C_3SiO(102.4 eV) [14,15]. The binding energy of Si2p peak of the SiOC/HfO_2 fibers is 1.2 eV higher than that of the PHfSO fiber because of the breakage of Si–C bonds and the formation of new Si–O bonds during pyrolysis. C1s peak (Fig.9c) shows a main peak at 285.0 eV for aromatic carbon environment [14,15] indicating free carbon in the fibers. The $Hf4f_{5/2}$ and $Hf4f_{7/2}$ peaks (Fig.9d) appear at 19.7 and 18.1 eV mainly assigned to HfO_2(IV) [16]. The shift of $Hf4f_{7/2}$ peak to higher binding energy from 17.5 to 18.1 eV can be attributed to the formation of hafnium silicate [16]. FTIR spectrum of the SiHfOC fibers shows a characteristic absorption band of SiOC glass with an intense broad peak at 1090 cm^{-1} for Si–O–Si stretching vibration and a peak at 823 cm^{-1} for Si–C stretching vibration, as shown in Fig. 5b. Therefore, the SiOC/HfO_2 fibers consist of mixed silicon oxycarbide (SiO_xC_{4-x}, x=1–4) and tetravalent hafnium-oxygen units embraced with some free carbon phase, similar with the hafnium modified PSO precursor derived SiOC/HfO_2 ceramics [5–8].

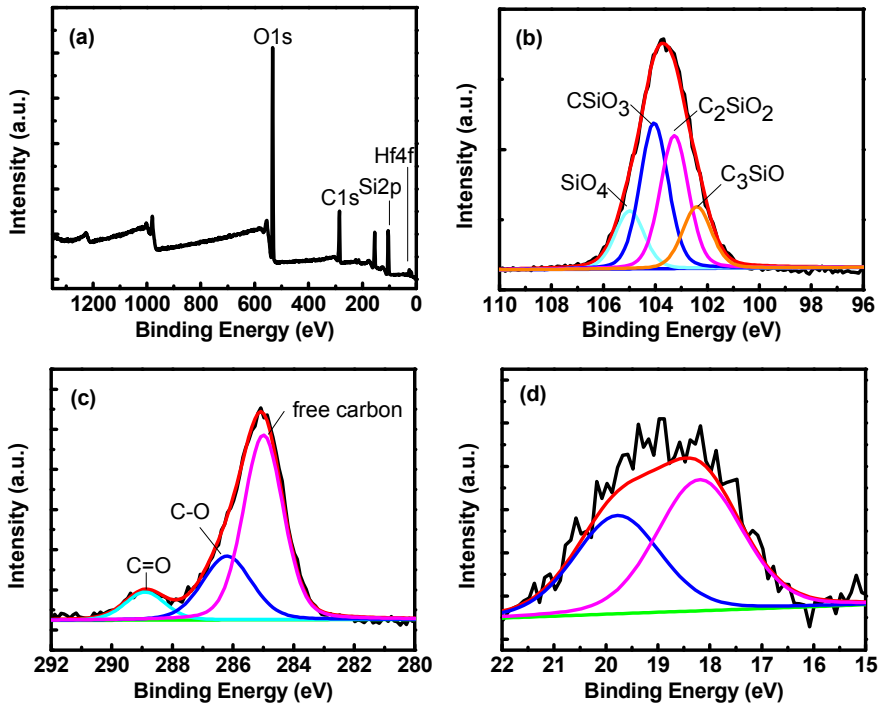

Fig.9 XPS spectrum of SiOC/HfO_2 fibers from PHfSO fibers pyrolyzed at 1000 °C for 1 h in argon (a) and their Si2p (b), C1s (c) and Hf4f (d) peak fittings.

The SiOC/HfO_2 fibers exhibit good mechanical properties measured by tensile tests. The maximum breaking force of up to

22 cN with corresponding tensile strength of 1.56 GPa is obtained from a fiber with diameter of 12 μm observed by SEM. The strength of the SiOC/HfO_2 fibers is higher than that of sol–gel derived SiOC fibers[13,20] and close to that of sol-gel derived silica fibers (highest strength 1.7 GPa [21]). Kamiya et al.[13] measured a large number of tensile strength of sol-gel derived SiOC fibers and attributed the scattered strength data of the hand-drawn fibers (0.1~1.2 GPa)to factors such as fiber diameter, unevenness surface, fiber twisting and accidental torsion during measurement[13]. Chen et al. [20] fabricated SiOC fibers from vinyltrimethoxysilane using secondary cellulose acetate as spinning reagent by sol–gel method, and the measured tensile strength is in the range of 184-940 MPa. The high strength of our fibers should arise from the dense structure of the fibers benefiting from the incorporation of Hf in the SiOC network.

The tensile strength of the SiOC/HfO_2 fiber is scattered as many other ceramic fibers (such as SiC, Al_2O_3 and SiO_2 fiber), which is mainly depends on fiber diameter. The thin fibers (diameter less than 12 μm) show high strengths with the average data of more than 500 MPa. However, if the fiber diameter is higher than 15 μm, the strength reduces to ~200 MPa. Griffith theory of brittle failure believes that the strength of brittle materials is governed by the initial presence of small cracks, and failure occurs when the most vulnerably oriented crack in a population of randomly oriented cracks begins to extend under the applied stress.[22] As the size of a brittle material grows, for instance 2-D fiber materials, the probability that it will fracture from a single crack increases. The SiOC/HfO_2 fibers exhibit single-stage stress–strain curve indicating its brittleness character (Fig.10), and its tensile strength is determined by various defects thus bringing out the polydispersity due to random distribution of defects. Therefore, fabrication of fine fibers is one of the effective approaches to further improve their strengths, and future work will be focused on the fabrication of small-diameter SiOC/HfO_2 fibers by further controlling the solution viscosity and spinning process.

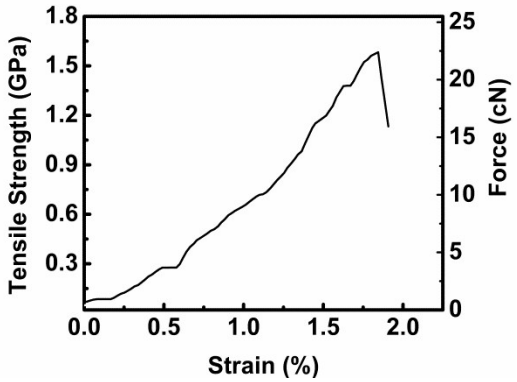

Fig.10 a stress–strain curve of SiOC/HfO_2 fibers from PHfSO fibers pyrolyzed at 1000 °C for 1 h in argon.

Conclusions

To conclude, continuous PHfSO gel fibers have been drawn from the optimized TEOS–DMDES–$HfOCl_2$-EtOH solution using PVP as spinning reagent, and subsequent pyrolysis gives out dense SiOC/HfO_2 fibers with high strength. The high strength of SiOC/HfO_2 fibers makes it possible to function as the basic and key reinforced materials for fabricating high performance ceramic matrix composites (CMCs) which are considered as the most promising candidates for (ultra)high-temperature structural components in energy, chemical and transportation industries. Moreover, this sol-gel process provides a simple and effective method to incorporate Hf into SiOC fibers which may expand to fabricate other multi–component high-temperature Si(M)OC fibers (M=B, Ti, Al and Zr et al.).

Acknowledgments

We thank Prof. Dr. Ya-li Li of Tianjin university of China for lab support. We acknowledge the funding supports from National Natural Science Foundation of China (Grant. No.: 51202157), Tianjin Research Program of Application Foundation and Advanced Technology (Grant. No.: 14JCQNJC02800), and Independent Innovation Foundation of Tianjin University (Grant. No.: 2013XQ–0004).

Notes and references

[a] *Key Laboratory of Advanced Ceramics and Machining Technology, Ministry of Education, School of Materials Science and Engineering, Tianjin University, Tianjin, 300072, China. Fax: 022-27402187; Tel: 022-27402187; E-mail: sudong@tju.edu.cn*

[b] *Guangdong Key Laboratory of Membrane Materials and Membrane Separation, Guangzhou Institute of Advanced Technology, Chinese Academy of Sciences, Guangzhou 511458, China, E-Mail: xiao.yan@giat.ac.cn*

1 S. Brahmandam, R. Raj, *J. Am. Ceram. Soc*. 2007, **90**, 3171.
2 R. Sujith, A.B. Kousaalya, R. Kumar, *J. Am. Ceram. Soc.* 2011, **94**, 2788.
3 B. Papendorf, K. Nonnenmacher, E. Ionescu, H.J. Kleebe, R. Riedel, *Small*. 2011, **7**, 970.
4 K. Terauds, D.B. Marshall, R. Raj, *J. Am. Ceram. Soc.* 2013, **96**, 1278.
5 E. Ionescu, B. Papendorf, H.J. Kleebe, F. Poli, K. Muller, R. Riedel, *J. Am. Ceram. Soc.* 2010, **93**, 1774.
6 E. Ionescu, B. Papendorf, H.J. Kleebe, R. Riedel, *J. Am. Ceram. Soc.* 2010, **93**, 1783.
7 H.J. Kleebe, K. Nonnenmacher, E. Ionescu, R. Riedel, *J. Am. Ceram. Soc.* 95(2012)2290.
8 K. Nonnenmacher, H.J. Kleebe, J. Rohrer, E. Ionescu, R. Riedel, *J. Am. Ceram. Soc.* 2013, **96**, 2058.
9 C. B. Jing, X. G. Xu, and J. X. Hou, *J. Sol-Gel Sci. Technol.*, 2008, 45, 109.
10 D.G. Yu, G.R. Williams, X. Wang, X.K. Liu, H.L. Li, S.W.A. Bligh, *RSC Adv.*, 2013, **3**, 4652.
11 S. Sakka, K. Kamiya, *J. Non–Cryst. Solids* 1982, **48**, 31.
12 K. Matsuzaki, D. Arai, N. Taneda, T. Mukaiyama, M. Ikemura, *J. Non–Cryst. Solids.* 1989, **112**, 437.
13 K. Kamiya, A. Katayama, H. Suzuki, K. Nishida, T. Hashimoto, J. Matsuoka, H. Nasu, *J. Sol–Gel. Sci. Technol.* 1999, **14**, 95.
14 G.D. Soraru, G. D.Andrea, A. Glisenti, Mater. Lett. 1996, **27**,1.
15 A. Karakuscu, R. Guider, L. Pavesi, G.D. Soraru, *J. Am. Ceram. Soc.* 2009, **92**, 2969.
16 T.C. Chen, C.Y. Peng, C.H. Tseng, *IEEE Trans. Electron Devices.* 2007, **54**, 759.
17 G. M. Renlund, S. Prochazka, and R.H. Doremus, *J. Mater. Res.* 1991, 6, 2716.
18 G. Trimmel, R. Badheka, F. Babonneau J., Latournerie, P. Dempsey, D. Bahloul-Houlier, et al. *J. Sol–Gel Sci. Technol.* 2003, **26**, 279.
19 V. Gualandris, D. Hourlier-Bahloul, F. Babonneau, *J. Sol–Gel Sci. Technol.*, 1999, **14**, 39.
20 L. F. Chen, Z. H. Cai, L. Zhang, et al. *J. Mater. Sci*., 2007, **42**, 1004.
21 T. Hashimoto, K. Kamiya, H. Nasu, *J. Non–Cryst. Solids.* 1992, **143**, 31.
22 A. Griffith, *Philos.Trans. R. Soc.* London Ser. A 1921, **221**, 163).